(Received 5 May 2023, Accepted 20 November 2023, Scheduled 26 November 2023)

Design of Choke Loaded Horn Antenna Offering Stable Phase Center for Fresnel Field Based Holography Measurement

Yogesh Tyagi, Pratik Mevada*, Dinesh K. Jangid,
Vijay K. Singh, Sanjeev Kulshrestha, and Milind B. Mahajan

Space Applications Centre (SAC), Indian Space Research Organization (ISRO), Ahmedabad, India

ABSTRACT: This paper introduces the new design of a choke loaded horn antenna, at 89.75 GHz for metrology of the large paneled reflector antenna using the Fresnel field based radio holography technique. The proposed choke loaded horn antenna offers the φ cut-wise extremely stable phase center (< 2 µm), which is required to obtain < 5 µm surface accuracy during holographic measurement. The design of choke loaded horn antenna has been presented along with its simulation performance and tolerance analysis. The antenna has been developed using a simple computer numerical control (CNC) milling process and characterized in the anechoic chamber. The measured and simulated results are also compared, and a good match has been achieved between the measured and simulated performances of the horn antenna.

1. INTRODUCTION

Radio holography technique is one of the widely popular best techniques for the panel alignment of the reflector antenna, especially functioning at high frequency [1–4]. Radio holography technique may be implemented by measuring the antenna in any one of the three radiation zones, namely, radiative nearfield, Fresnel field, and far field zone [5]. The basic flow is to generate the aperture field distribution and then compute the reflector surface error profile using the half path length (HPL) concept [1]. Typically, such a radio holography technique is used for reflector antenna in prime focal geometry, where a feed is kept at the focal point of the reflector. Holography technique can offer ≤ 5 µm surface error accuracy. Ideally, the feed used for such measurement should be designed to yield a stable phase center and radiation pattern having azimuthal amplitude and phase symmetry. When Fresnel field based radio holography is implemented, the feed is axially displaced from the focal point to compensate for the nearfield terms [6]. Moreover, the feed phase is directly added to the surface error. Any error pattern in the farfield phase of the feed leads to a similar error pattern on the surface error profile. Usually, the phase center variation over the φ cuts is expected in the feed design, which subsequently results in the astigmatism error on the surface error profile. Therefore, it is required to design the feed with a highly stable phase center over φ cuts to achieve micron-order surface error accuracy.

The design of a feed offering a stable phase center is one of the most challenging tasks. The widely known type of horn antenna offering such characteristics is corrugated horn [7–9]. However, the fabrication of such a horn antenna is complicated and requires meticulous mechanical design and complicated fabrication technology including micromachining. The conventional circular feed horn integrated with a dielectric lens may also be designed [10–12]. Its major drawback is that the dielectric properties usually need to be accurately known at this band of frequency; otherwise, it results in a de-tuned performance. Choke loaded horn antenna is one of the widely used horns, mainly for reflector feeds and global navigation satellite system (GNSS) related systems. Adding the choke ring at the throat section of the horn controls the surface wave propagation on the aperture surface, which can be used for various types of pattern synthesis. X-band choke ring horn antenna has been designed, developed, and characterized for NASA's SWOT mission by Chahat et al. [13]. Here, the choke ring based horn design has been selected to achieve low cross polarization level and multipath interference. In [14], Fallahzadeh et al. presented a descending stepped choke ring antenna at the X-band for LEO satellites. The loading of choke rings is used to achieve a wide radiation pattern to cover the 125° angular range for LEO satellites. The analysed and measured radiation pattern performance of the antenna in the presence of the mock-up structure of the satellite has also been discussed. In [15], Taghdidi et al. presented an interesting structure called a dual-band double folded substrate integrated choke ring (DFSICR), which can be used for multipath mitigation over the GNSS frequency bands. Such a structure offers a low profile, light weight, and easy fabrication. Papers are also reported describing the phase center stable antennas and their requirements in millimeter wave band [16, 17]. However, the designs presented in [16, 17] are not evaluated for the φ cut-wise phase center.

In this manuscript, we present the design, development, and characterization of a choke loaded horn antenna explicitly designed for Fresnel field-based radio holography for surface error profile extraction of paneled reflector antenna. Here, the Fresnel field based holography is performed at 89.75 GHz. The design and development of horn antenna at such high frequency limit the prospective design variants, and the most convenient

* Corresponding author: Pratik Mevada (mevadapratik@gmail.com).

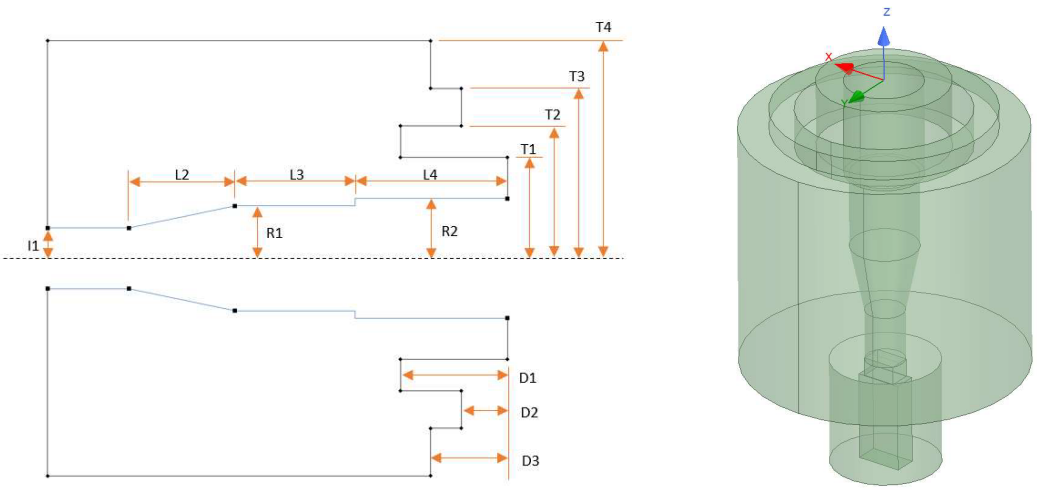

FIGURE 1. Geometry of choke loaded horn antenna.

	Dimension (mm)	Tolerance (μm)
$I1$	1.1	±5
$T1$	3.64	±30
$T2$	4.78	±30
$T3$	6.13	±30
T4	7.8	±50
$D1$	3.87	±30
$D2$	1.67	±30
$D3$	2.78	±50

TABLE 1. Feed horn dimensions and tolerances.

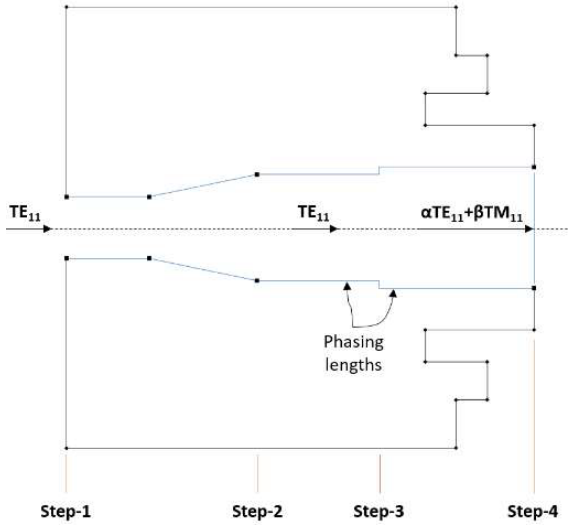

FIGURE 2. Step wise approach for the proposed horn antenna.

of them is the choke ring loading on the throat of a conventional multimode horn antenna, as compared to the other complicated variants, including corrugated horn antenna. Here, specific attention has been given to the design of the choke ring structure to modify the aperture surface currents, such that it offers φ cut stable phase center. To the best of the authors' knowledge, such a phase center stable choke horn design is not available in the open literature. In Section 2 of the manuscript, the design and modelling geometry of the feed are discussed. Section 3 contains the simulated and measured results of the developed feed. Section 4 concludes the manuscript.

2. GEOMETRY AND DESIGN OF CHOKE LOADED HORN

Figure 1 shows the proposed choke loaded horn antenna with dimensional details. A two-step internal cavity has been used to excite $\alpha\text{TE}_{11} + \beta\text{TM}_{11}$ modes, which can form the fundamental HE_{11} hybrid mode, by adjusting the α and β mode contents. The α and β parameters are usually optimized such that the TE and TM modes travel with the same phase velocity, coinciding with the phase centers in the E and H planes [18]. Here, the optimized values for the mode content are ($\alpha = 0.327$ dB) and ($\beta = -12.17$ dB). Moreover, the mode purity of HE_{11} is significantly affected by edge currents, which alters the phase center in the different φ planes. Therefore, the annular ring type choke is introduced at the horn aperture, which suppresses the outer wall currents created by the surface waves and maintains the φ cut-wise phase center. In addition, the choke structure also reduces the back lobe in the radiation pattern. Fig. 2 shows the stepwise approach for the design, and the design steps are as follows in brief. The length and width of the choke rings have been optimized using the global optimization algorithm available in TICRA CHAMP [19] with the goal to achieve the stable φ cut-wise phase center over the 64° annular range.

Step-1: Selection of diameter of input waveguide such that it supports only dominant TE_{11} mode and is compatible with back waveguide routing

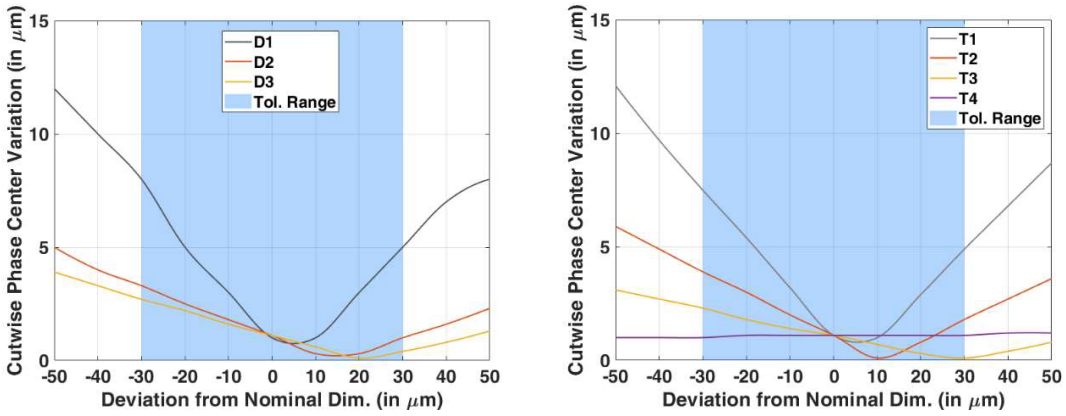

FIGURE 3. Plot of variation of φ cut-wise phase center with ± 50 µm variation in $D1$, $D2$, $D3$, $T1$, $T2$, $T3$ and $T4$ dimensions.

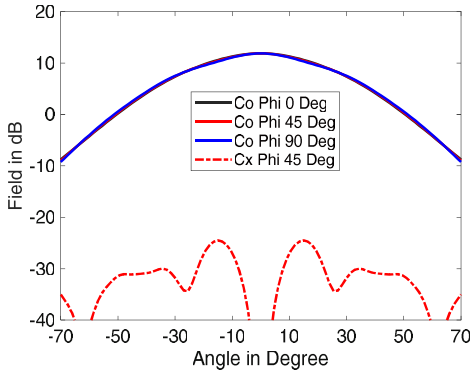

FIGURE 4. Simulated far field radiation pattern of choke loaded horn antenna at 89.75 GHz.

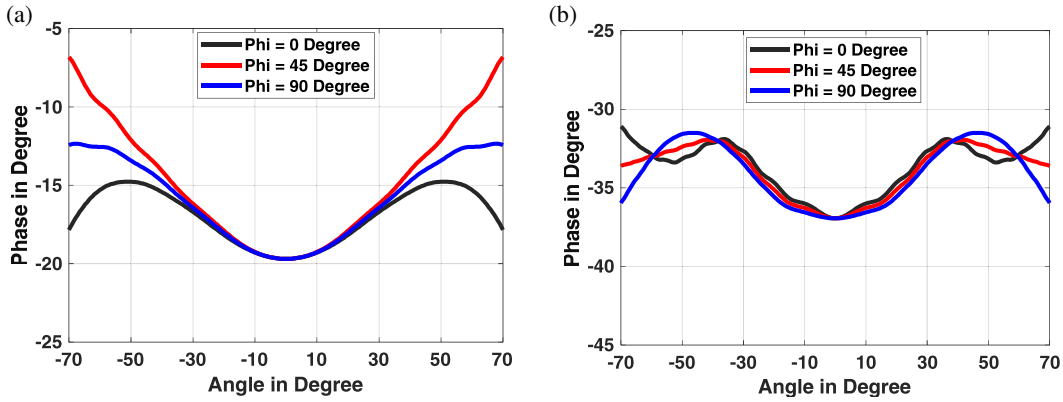

FIGURE 5. Far field phase plot at 89.75 GHz of horn antenna (a) without choke loading and (b) with choke loading.

TABLE 2. Variation of phase center (in microns) with frequency for horn antenna without choke loading.

Frequency (in GHz)	$\varphi = 0°$ Cut	$\varphi = 45°$ Cut	$\varphi = 90°$ Cut	Variation over φ cuts
89.55	-175.4	-140.3	-104.1	71.3
89.65	-163.9	-134.1	-103.3	60.6
89.75	-152.5	-127.9	-102.4	50.1
89.85	-141.1	-121.7	-101.6	39.5
89.95	-129.5	-115.5	-100.7	28.8

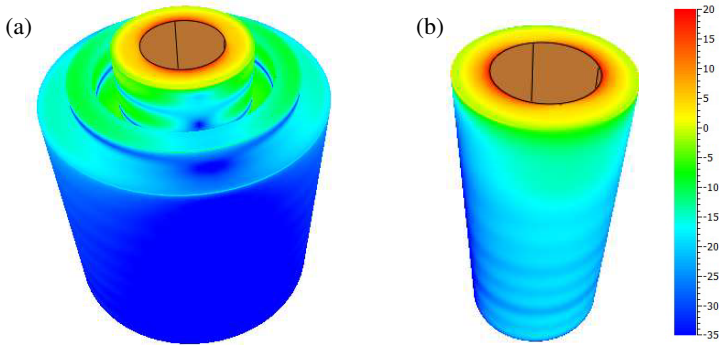

FIGURE 6. Field distribution of the horn (a) with and (b) without choke loading.

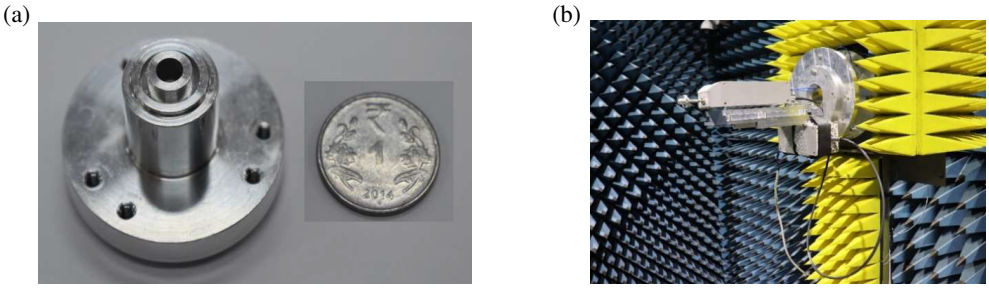

FIGURE 7. (a) Developed choke loaded feed horn antenna, and (b) mounting of the feed horn antenna in anechoic chamber.

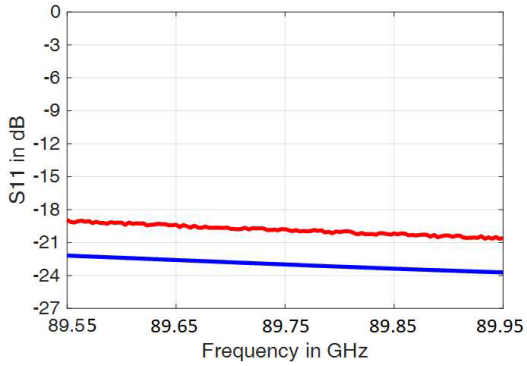

FIGURE 8. Simulated (in blue) and measured (in red) reflection coefficient.

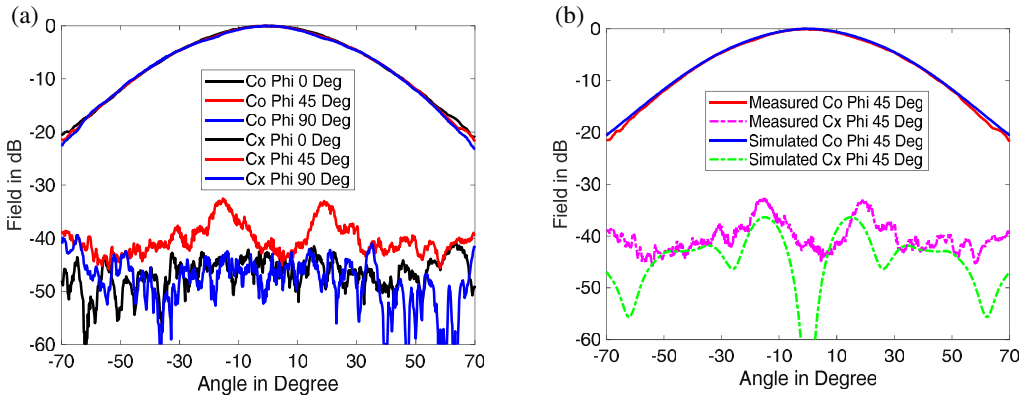

FIGURE 9. (a) Measured radiation pattern at 89.75 GHz and (b) comparison of simulated and measured radiation pattern at 89.75 GHz.

Step-2: Flare the circular section to improve the reflection property of the dominant TE_{11} mode

TABLE 3. Variation of phase center (in microns) with frequency for horn antenna with choke loading.

Frequency (in GHz)	$\varphi = 0°$ Cut	$\varphi = 45°$ Cut	$\varphi = 90°$ Cut	Variation over φ cuts
89.55	−140.8	−129.9	−118.6	22.2
89.65	−129.7	−124.0	−118.1	11.6
89.75	−118.8	−118.1	−117.1	1.7
89.85	−107.5	−112.3	−117.5	9.5
89.95	−96.4	−106.4	−116.4	20.0

Step-3: Azimuthal symmetry step to generate a combination of TE_{11} and TM_{11} modes in $\alpha : \beta$ ratio to achieve

- Pattern symmetry
- Reduce the cross-polarized field

Step-4: Add the choke rings to suppress the surface current, which disturbs the φ cut-wise phase center variation

Here, a standard rectangular port of WR-10 to circular waveguide transition has also been designed to feed the horn. The integrated performance of the horn with transition has been simulated using Ansys Electronics desktop 2022 R1 [20].

The tolerance analysis, being one of the most crucial steps before loading the RF design for mechanical fabrication, is presented in Fig. 3. Here, the plots showing the impact of variation in the sensitive dimensions of the horn on the φ cut-wise phase center variation are shown. From Fig. 3, it can be observed that ± 30 µm variation in the '$D1$' and '$T1$' dimensions results in 9 µm and 8 µm variation in the phase center, respectively. Hence, '$D1$' and '$T1$' are sensitive variables and need special attention during manufacturing.

3. SIMULATION AND MEASURED RESULTS

The simulated reflection coefficient $S_{11}\,(\text{dB}) < -22\,\text{dB}$ has been achieved over the 89.5 GHz to 90.5 GHz band. As depicted in Fig. 4, the simulated radiation pattern at 89.75 GHz shows a very good beam symmetry and very low cross-polarization performance. The proposed choke loaded horn offers a highly stable phase center over φ. Fig. 5 shows the far-field phase plot at 89.75 GHz for $\varphi = 0°$, 45° & 90° cuts of the horn antenna with and without choke. The phase center of the feed horn is computed considering $\theta = 64°$ angular range over the frequency band. The phase centers for $\varphi = 0°$, 45° & 90° cuts are listed in Tables 2 & 3 for the horn antenna without choke loading and with choke loading, respectively. From Tables 2 and 3, it can be observed that the choke loaded horn shows ≤ 2 µm variation in the phase center at 89.75 GHz, which is significantly less than the 50 µm variation in the phase center of the horn without choke loading. Here, Fig. 6 shows the current distribution on the horn antenna in the cases with and without choke loading. By comparing the current densities, it can be concluded that the choke loading has significantly altered the current density at the aperture plane.

The fabrication of choke loaded horn at 89.75 GHz calls for tight tolerances on the dimensions. An extensive sensitivity analysis has been carried out, and the required tolerances are derived and presented in Table 1 along with the design dimensions. The fabrication of the choke loaded horn antenna has been carried out using the computer numerical control (CNC) milling process, and Fig. 7(a) shows the image of the developed choke loaded feed horn antenna. The reflection coefficient measurement of the horn antenna has been carried out using Agilent E8363B microwave network analyser, and the measured result is compared with simulated ones in Fig. 8. Here measured reflection coefficient is < -18 dB. A minor discrepancy between simulated and experimental results can be observed, attributed to the dimensional deviation of the step above the given tolerance range for WR-10 to circular waveguide transition. The radiation pattern measurement of the antenna has been carried out in an anechoic chamber. The mounting condition of the antenna is shown in Fig. 7(b). Fig. 9(a) shows the measured radiation pattern of the developed feed horn at 89.75 GHz, and Fig. 9(b) compares the simulated and measured radiation patterns at 89.75 GHz. From Fig. 9(b), a good match between simulation and measurement has been achieved. Moreover, measured cross-polarization is < -32 dB, and excellent pattern symmetry has also been achieved.

4. CONCLUSION

In this manuscript, the design of a choke loaded horn antenna has been presented. The proposed antenna is designed to offer azimuth cut-wise extremely stable phase center at 89.75 GHz frequency over 64° angular conical range. It has been shown that the horn antenna without choke offers 50 µm variation in the φ cut-wise phase center. However, the phase center is stabilized to 2 µm by introducing and optimizing the choke around the horn throat. A rigorous sensitivity analysis has also been carried out to define the required fabrication tolerances on the dimensions and included in the manuscript. The proposed horn antenna has been fabricated using a simple milling process, making it best suitable for general designs at millimeter wave band. The developed horn antenna has been characterized in an anechoic chamber, and the measured results are presented with simulated ones. The comparison plots of the simulated and measured results show a good correlation.

The developed choke horn antenna will be used for the metrology of the large reflector antenna being developed at SAC, ISRO, Ahmedabad for the THz telescope.

ACKNOWLEDGEMENT

The authors wish to thank Shri N. M. Desai, Director, SAC for his support and encouragement during this work. The authors would also like to thank all the engineers of the Microwave Sensors Antenna Division (MSAD) and Antenna Measurement and Test Division (AMTD) for their help extended.

REFERENCES

[1] Bennett, J., A. Anderson, P. McInnes, and A. Whitaker, "Microwave holographic metrology of large reflector antennas," *IEEE Transactions on Antennas and Propagation*, Vol. 24, No. 3, 295–303, 1976.

[2] Hunter, T. R., F. R. Schwab, S. D. White, J. M. Ford, F. D. Ghigo, R. J. Maddalena, B. S. Mason, J. D. Nelson, R. M. Prestage, J. Ray, P. Ries, R. Simon, S. Srikanth, and P. Whiteis, "Holographic measurement and improvement of the green bank telescope surface," *Publications of the Astronomical Society of the Pacific*, Vol. 123, No. 907, 1087–1099, Sep. 2011.

[3] Usoff, J., M. Clarke, and et al., "Optimizing the HUSIR antenna surface," *Lincoln Laboratory Journal*, Vol. 21, No. 1, 83–105, 2014.

[4] Lopez-Perez, J. A., P. de Vicente Abad, J. A. Lopez-Fernandez, F. Tercero Martinez, A. Barcia Cancio, and B. Galocha Iragueen, "Surface accuracy improvement of the Yebes 40 meter radiotelescope using microwave holography," *IEEE Transactions on Antennas and Propagation*, Vol. 62, No. 5, 2624–2633, May 2014.

[5] Balanis, C., *Modern Antenna Handbook*, Wiley, Somerset, 2011.

[6] Baars, J. W. M., R. Lucas, J. G. Mangum, and J. A. Lopez-Perez, "Near-field radio holography of large reflector antennas," *IEEE Antennas and Propagation Magazine*, Vol. 49, No. 5, 24–41, Oct. 2007.

[7] McElhinney, P., C. R. Donaldson, L. Zhang, and W. He, "A high directivity broadband corrugated horn for W-band gyrodevices," *IEEE Transactions on Antennas and Propagation*, Vol. 61, No. 3, 1453–1456, Mar. 2013.

[8] Eleftheriades, G., W. Ali-Ahmad, L. Katehi, and G. Rebeiz, "Millimeter-wave integrated-horn antennas. I. Theory," *IEEE Transactions on Antennas and Propagation*, Vol. 39, No. 11, 1575–1581, Nov. 1991.

[9] Ali-Ahmad, W., G. Eleftheriades, L. Katehi, and G. Rebeiz, "Millimeter-wave integrated-horn antennas. II. Experiment," *IEEE Transactions on Antennas and Propagation*, Vol. 39, No. 11, 1582–1586, Nov. 1991.

[10] Poyanco, J.-M., F. Pizarro, and E. Rajo-Iglesias, "Cost-effective wideband dielectric planar lens antenna for millimeter wave applications," *Scientific Reports*, Vol. 12, No. 1, Mar. 10, 2022.

[11] Konstantinidis, K., A. P. Feresidis, C. C. Constantinou, E. Hoare, M. Gashinova, M. J. Lancaster, and P. Gardner, "Low-THz dielectric lens antenna with integrated waveguide feed," *IEEE Transactions on Terahertz Science and Technology*, Vol. 7, No. 5, 572–581, Sep. 2017.

[12] Zhang, B., Y.-X. Guo, Q. Guo, L. Wu, K. B. Ng, H. Wong, Y. Zhou, and K. Huang, "Dielectric and metallic jointly 3D-printed mmWave hyperbolic lens antenna," *IET Microwaves Antennas & Propagation*, Vol. 13, No. 11, 1934–1939, Sep. 11, 2019.

[13] Chahat, N., L. R. Amaro, J. Harrell, C. Wang, P. Estabrook, and S. A. Butman, "X-band choke ring horn telecom antenna for interference mitigation on NASA's SWOT mission," *IEEE Transactions on Antennas and Propagation*, Vol. 64, No. 6, 2075–2082, Jun. 2016.

[14] Fallahzadeh, M., H. Aliakbarian, A. Haddadi, and S. Radiom, "Beam shaping of X-band stepped choke ring antenna for LEO satellite applications," *IEEE Aerospace and Electronic Systems Magazine*, Vol. 33, No. 10, 34–39, Oct. 2018.

[15] Taghdisi, E., M. S. Ghaffarian, and R. Mirzavand, "Low-profile substrate integrated choke rings for gnss multipath mitigation," *IEEE Transactions on Antennas and Propagation*, Vol. 70, No. 3, 1706–1718, Mar. 2022.

[16] Fernandes, C. A., E. B. Lima, and J. R. Costa, "Broadband integrated lens for illuminating reflector antenna with constant aperture efficiency," *IEEE Transactions on Antennas and Propagation*, Vol. 58, No. 12, 3805–3813, Dec. 2010.

[17] Ignatenko, M., B. Sitnakauskas, M. Notaros, and D. S. Filipovic, "A phase center-stabilized K/Ka/V-band linearly polarized horn for luneburg lenses," *IEEE Antennas and Wireless Propagation Letters*, Vol. 16, 2726–2729, 2017.

[18] Olver, A., "Microwave horns and feeds," Institution of Electrical Engineers, London, 1994.

[19] TICRA CHAMP. [Online]. Available: https://www.ticra.com/software/champ3d.

[20] Ansys HFSS. [Online]. Available: https://www.ansys.com/en-in/products/electronics/ansys-hfss.